[16]D. G. Shirk, S. Fiarman, N. Y. Wei, and H. M. Kuan, Bull. Am. Phys. Soc. 11 16, 489 (1971); H. M. Kuan, private communication.
[17]E. C. Halbert and J. B. French, Phys. Rev. 105, 1563 (1957).
[18]A. P. Zuker, B. Buck, and J. B. McGrory, Phys. Rev. Letters 21, 39 (1968).
[19]S. Lie, T. Engeland, and G. Dahll, Nucl. Phys. 156, 449 (1970).
[20]S. Lie and T. Engeland, to be published.
[21]A. Gallman, F. Jundt, E. Aslanides, and D. E. Alburger, Phys. Rev. 179, 921 (1969).
[22]B. Lawergren and I. V. Mitchell, Nucl. Phys. A98, 481 (1967).
[23]G. W. Phillips and W. W. Jacobs, Phys. Rev. 184, 1052 (1969).
[24]C. E. Steerman and F. C. Young, Bull. Am. Phys. Soc. 15, 529 (1970).
[25]J. P. Allen and G. W. Phillips, Annual Report, Nuclear Physics Laboratory, University of Washington, Seattle, 1967 (unpublished), p. 37.
[26]R. L. McGrath, Phys. Rev. 145, 802 (1966).
[27]A. P. Shukla and G. E. Brown, Nucl. Phys. A112, 296 (1968).
[28]G. E. Brown and A. M. Green, Nucl. Phys. 25, 401 (1966).
[29]O. D. Brill, A. D. Vongai, and A. A. Ogloblin, Izv. Akad. Nauk SSSR, Ser. Fiz. 33, 615 (1969) [transl.: Bull. Akad. Sci. USSR, Phys. Ser. 33, 567 (1969)].
[30]E. Adelberger and A. Nero, Progress Report, tandem Van de Graaff accelerator, Stanford University, 1968–1969 (unpublished), p. 44.

PHYSICAL REVIEW C VOLUME 5, NUMBER 2 FEBRUARY 1972

Two-Nucleon Interactions, the Unitary Model, and Polarization in Elastic Nucleon-Deuteron Scattering*

S. C. Pieper and K. L. Kowalski
Department of Physics, Case Western Reserve University, Cleveland, Ohio 44106
(Received 26 July 1971)

The use of the first-order unitary model to calculate nucleon polarizations in elastic nucleon-deuteron scattering at energies up to 40 MeV is investigated. One shortcoming of extant unitary-model calculations, that of inadequate two-nucleon input, is partially remedied by introducing a variety of more realistic models for the two-nucleon interaction. It is found that even with the latter interactions the unitary model fails to represent the nucleon polarization, and, as is to be expected from the work of Sloan *et al.*, to a lesser degree, the elastic differential cross section. The nucleon polarization is found to be extremely sensitive even at fairly low energies to the presence of the P-wave components of the two-nucleon amplitudes when the three-particle scattering is computed via the unitary and other approximations. This indicates that any method (exact or otherwise) for computing polarizations in N-d scattering must include these components.

I. INTRODUCTION

Recently calculations of the differential cross section and nucleon polarization in elastic nucleon-deuteron scattering were carried out over an energy range from 11 to 40 MeV using an approximate K-matrix formalism.[1-4] The results obtained were quite remarkable considering the crude two-nucleon input used and the approximations made to the three-particle dynamics. It now appears that the calculations of KK[1,2] are incorrect.

The latter circumstance was first pointed out by Aarons and Sloan.[5] Their primary (and correct) objection against the computational procedure in KK concerns a premature truncation in the total angular momentum J. However, even granting such a truncation ($J \leq \frac{3}{2}$) the results of KK appear to be unreproducible with the prescribed two-nucleon input.[5,6] The computations to be described in the present work substantiate the conclusions of Aarons and Sloan on both of these issues.

When sufficient partial-wave states are included to ensure convergence with respect to J, the N-d polarization predicted with the N-N interaction of KK is, as is shown in Ref. 5 and the present paper, essentially zero. In order to determine the cause of this complete disagreement with the experimental results, we have computed N-d polarizations and cross sections in the unitary model using a variety of more realistic N-N input. We conclude that even with a fairly complete representation of the N-N amplitudes (S, P, and D waves) the Sloan approximation fails to give qualitatively correct results for the N-d polarization. Although the structure of the elastic differential cross section is reasonably reproduced, the magnitude of the forward peak is, as is to be expected from the work of Sloan,[4] poorly estimated.

Furthermore, the strong dependence of our results on the inclusion of P-wave N-N potentials indicates that any attempt to calculate the N-d polarizations even at low energies should include a representation of these amplitudes. This result is perhaps not surprising in view of the fact that the Yamaguchi[7] tensor potentials used in Ref. 5 and KK predict polarizations in N-N scattering which are identically zero.

In Sec. II we present the particular angular momentum analysis of the K-matrix equations associated with the Sloan approximation used in the present work. Section III contains a detailed description of the various N-N potentials utilized and the results obtained with these interactions in the Sloan approximation to elastic N-d scattering. The final section is devoted to a summary of the conclusions of this work.

II. SLOAN APPROXIMATION

In this section we give the angular momentum decomposition used in connection with the present computations. This analysis is considerably more sophisticated than that used in KK and results in a marked reduction of computer time. Our results are similar to, but not exactly the same as, those obtained by Sloan[8] in his reduction of the Faddeev-Lovelace equations[9,10] for the Yamaguchi[7] potentials. To get the equation analogous to (2.24), one has to iterate the equations in Ref. 8 once.[5] The

TABLE I. Potential sets used in the calculations. The units are such that $\hbar = 1$ fm $= 1$ MeV $= 1$. In these units $m = 0.024\,129$ MeV^{-1} fm^{-2}.

Set	$^1S_0$	$^3S_1$	$^3S_1$-$^3D_1$	$^1P_1{}^3P_0{}^3P_1{}^3P_2$	$^1D_2{}^3D_1{}^3D_2{}^3D_3$
		Designation of potentials used for each channel			
K	1SK	...	3ST	...	...
A	1SA	...	3ST	P1	...
B	1SA	...	3ST	P2	...
C	1SA	3SC	...	P2	...
D	1SA	3SC	...	P2	D1

$^1S_0$ potentials

Designation	$\lambda^{1,0}_{0,0}$ (MeV/fm)	$\gamma^{1,0}_{0,0}$ (fm^{-1})	a (fm)	r_e (fm)
1SK	−98.469	1.2623	20.34	2.50
1SA	−72.600	1.1438	19.95	2.78

$^3S_1$, $^3S_1$-$^3D_1$ potentials

Designation	$\lambda^{0,1}_1$ (MeV/fm)	γ_c (fm^{-1})	γ_t (fm^{-1})	r	E_D (MeV)	% D state	Q (fm^2)	a (fm)	r_e (fm)
3SC	−205.38	1.4224	...	0	−2.226	0	0	−5.40	1.74
3ST	−73.814	1.2390	1.9520	−4.5400	−2.226	7.02	0.2825	−5.40	1.72

P-wave potentials

Channel	P1 $\lambda^{I,S}_{1,j}$ (MeV/fm)	P1 $\gamma^{I,S}_{1,j}$ (fm^{-1})	P2 $\lambda^{I,S}_{1,j}$ (MeV/fm)	P2 $\gamma^{I,S}_{1,j}$ (fm^{-1})
$^1P_1$	3021.4	2.7082	925.97	2.3910
$^3P_0$	−27.369	0.903 59	−29.324	0.919 22
$^3P_1$	177.01	1.3068	36.569	0.972 45
$^3P_2$	−313.23	1.8759	−196.19	1.7024

D-wave potential

Channel	D1 $\lambda^{I,S}_{2,j}$ (MeV/fm)	D1 $\gamma^{I,S}_{2,j}$ (fm^{-1})
$^1D_2$	−8.8032	0.854 43
$^3D_1$	67.491	0.935 94
$^3D_2$	−62.676	0.931 12
$^3D_3$	−22.591	1.2551

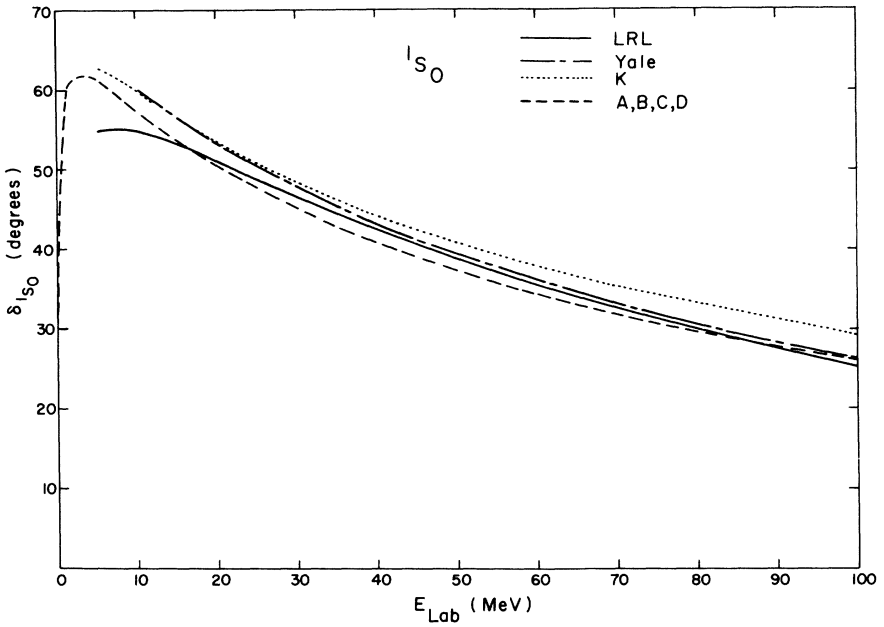

FIG. 1. N-N $^1S_0$ phase shifts. The solid line is the Livermore VII–IX energy-dependent analysis (Ref. 17); the dash-dot line is the Yale Y-IV n-p analysis (Ref. 16), the dotted line is for potential Set K, while the dashed line is Sets A–D. Phase shifts are in Stapp nuclear barred notation (Ref. 18).

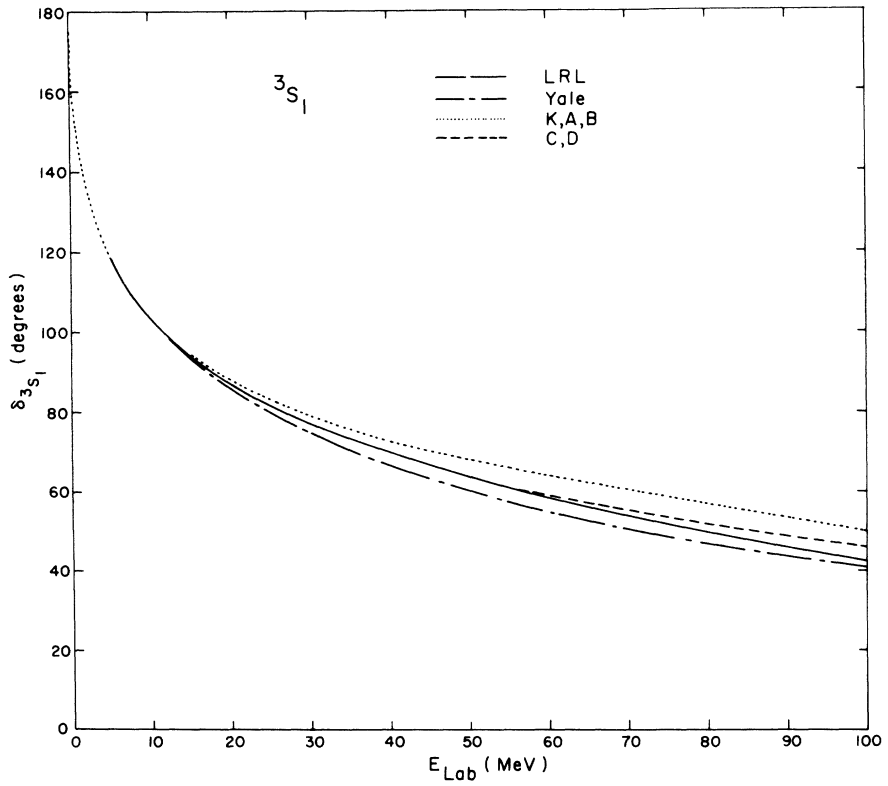

FIG. 2. $^3S_1$ phase shifts. The dotted line is K, A, B; dashed line is C, D.

computational difficulties in the two formulisms are essentially the same.

In the following equations we assume three identical nucleons whose wave function is totally antisymmetric in spin-isospin-coordinate space. The reader is referred to KK for a general description of the Sloan approximation[4] and the steps leading to equations (2.1) and (2.3).

The partial-wave form of the K matrix for elastic N-d scattering is

$$U^J(l',S'|l,S)=\bar{U}^J(l',S'|l,S)-i\frac{\pi}{2}\frac{4m}{3}q \times\sum_{l''S''}\bar{U}^J(l',S'|l'',S'')U^J(l'',S''|l,S)\,. \tag{2.1}$$

Here $U^J(l',S'|l,S)$ and $\bar{U}^J(l',S'|l,S)$ are, respectively, the partial-wave decompositions of the elastic N-d transition matrix and reduced K matrix as defined in KK:

$$\langle S',m_S'|\,U(\vec{q}'|\vec{q})|\,S,m_S\rangle =\sum\left\langle\begin{matrix}S' & l'\\ m_S' & m_l'\end{matrix}\middle|\begin{matrix}J\\ M\end{matrix}\right\rangle\left\langle\begin{matrix}S & l\\ m_S & m_l\end{matrix}\middle|\begin{matrix}J\\ M\end{matrix}\right\rangle \times Y_{l',m_l'}(\vec{q}')Y_{l,m_l}(\vec{q})U^J(l',S'|l,S)\,. \tag{2.2}$$

The Clebsch-Gordan coefficients are in the notation of Sharp and von Baeyer[11] and are related to those of Blatt and Weisskopf[12] by

$$\left\langle\begin{matrix}j_1 & j_2\\ m_1 & m_2\end{matrix}\middle|\begin{matrix}J\\ M\end{matrix}\right\rangle=C_{j_1,j_2}(J,M;m_1,m_2)\,.$$

The momenta $\vec{q}$ and $\vec{q}'$ are the incoming and outgoing momenta of the nucleon measured in the three-body c.m. system and m is the nucleon mass. As discussed in KK, with the introduction of parity conservation, Eq. (2.1) corresponds to a set of two linear equations for the $J=\frac{1}{2}$ states and to three linear equations for the $J\geq\frac{3}{2}$ states.

The Sloan approximation consists of using the exchange and impulse graphs for the reduced K matrix elements:

$$\bar{U}^J(l',S'|l,S)=2\langle l',S',J;2|(W-H_0)|\,l,S,J;1\rangle +2\langle l',S',J;1|\bar{t}_2|\,l,S,J;1\rangle +2\langle l',S',J;3|\bar{t}_2|\,l,S,J;1\rangle, \tag{2.3}$$

where $|\,l,S,J;i\rangle$ denotes a state consisting of particle i incident with orbital angular momentum l upon the bound state (deuteron) of particles j and k (i,j,k cyclic). $\bar{t}_i$ is the two-nucleon transition operator for particles j and k with the Dirac-δ-function part of the bound-state pole subtracted out; it is evaluated at the customary Faddeev[9] parametric energy $E=W-3q_i^2/4m$. The kinetic energy operator is denoted by H_0.

A. Separable N-N Potentials

In this paper we will represent the N-N potentials by rank-one separable potentials acting in each two-nucleon angular momentum state. For

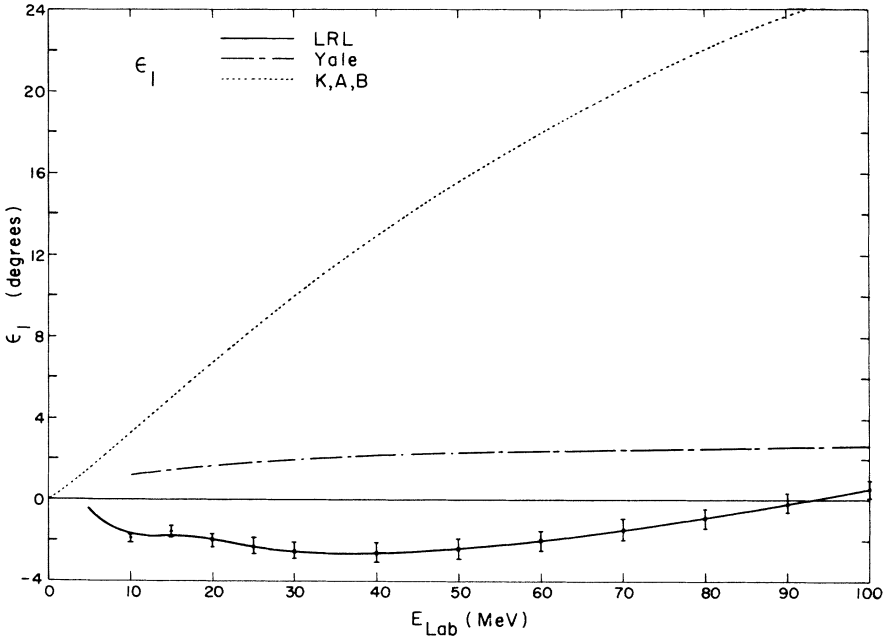

FIG. 3. ϵ_1 mixing parameter. The dotted line is Sets A, B, and K. $\epsilon_1=0$ for Sets C and D.

the $j=1$ isosinglet force we will use a tensor form:

$$\langle S=1, m_S'; I=0; \vec{p}' | V_{j=1}^{I=0,\,S=1} | S=1, m_S; I=0; \vec{p} \rangle = \lambda_1^{0,1} \sum_M v_{1;M}^{0,1}(m_S', \vec{p}') v_{1,M}^{0,1}(m_S, \vec{p}), \tag{2.4}$$

where

$$v_{1;M}^{0,1}(m_S, \vec{p}) = \delta_{M,m_S} Y_{00}(\vec{p}) u_{0,1}^{0,1}(p) + \sum_{m_l} \left\langle \begin{matrix} 1 & 2 \\ m_S & m_l \end{matrix} \middle| \begin{matrix} 1 \\ M \end{matrix} \right\rangle Y_{2,m_l}(\vec{p}) u_{2,1}^{0,1}(p). \tag{2.5}$$

The form factors u will be specified in Sec. III. For all other angular momentum and isospin states we will use central potentials

$$\langle S, m_S'; I, I_z; \vec{p}' | V_{l,j}^{I,S} | S, m_S; I, I_z; \vec{p} \rangle = \lambda_{l,j}^{I,S} \sum_M v_{l,j;M}^{I,S}(m_S', \vec{p}') v_{l,j;M}^{I,S}(m_S, \vec{p}), \tag{2.6}$$

with

$$v_{l,j;M}^{I,S}(m_S, \vec{p}) = \sum_{m_l} \left\langle \begin{matrix} S & l \\ m_S & m_l \end{matrix} \middle| \begin{matrix} J \\ M \end{matrix} \right\rangle Y_{lm_l}(\vec{p}) u_{l,j}^{I,S}(p). \tag{2.7}$$

As is well known, the N-N transition matrices for (2.6) and (2.7) are

$$\langle m_S', \vec{p}' | t_{l,j}^{I,S}(E) | m_S, \vec{p} \rangle = \lambda_{l,j}^{I,S} \frac{1}{g_{l,j}^{I,S}(E)} \sum_M v_{l,j;M}^{I,S}(m_S', \vec{p}') v_{l,j;M}^{I,S}(m_S, \vec{p}), \tag{2.8}$$

$$g_{l,j}^{I,S}(E) = 1 - m\lambda_{l,j}^{I,S} \int_0^\infty p^2 dp \frac{[u_{l,j}^{I,S}(p)]^2}{mE - p^2 + i\epsilon}. \tag{2.9}$$

For the $j=1$ isosinglet states the transition matrix is of the form (2.8) with $g_1^{0,1}(E)$ given by

$$g_1^{0,1}(E) = 1 - m\lambda_1^{0,1} \int_0^\infty p^2 dp \frac{[u_{0,1}^{0,1}(p)]^2 + [u_{2,1}^{0,1}(p)]^2}{mE - p^2 + i\epsilon}. \tag{2.10}$$

The deuteron bound-state wave function for the potential (2.4), (2.5) is

$$\phi_M(m_S, \vec{p}) = N \frac{v_{1;M}^{0,1}(m_S, \vec{p})}{E_D - p^2/m}, \tag{2.11}$$

where

$$\frac{1}{N^2} = \int_0^\infty p^2 dp \frac{[u_{0,1}^{0,1}(p)]^2 + [u_{2,1}^{0,1}(p)]^2}{(E_D - p^2/m)^2}, \tag{2.12}$$

and $E_D < 0$ is the deuteron bound-state energy.

B. Partial-Wave Analysis

With this preparation we can now evaluate the matrix elements in (2.3). We will sketch the analysis for the contribution of a central N-N interaction (2.6)–(2.9) to the term $\langle l', S', J; 1 | \bar{t}_2 | l, S, J; 1 \rangle$ and then state the results for the other cases. Completely written out this matrix element is

$$\begin{aligned}
&\langle l', S', J; 1 | \bar{t}_{L_n, j_n}^{I_n, S_n}\left(W - \frac{3q_2^2}{4m}; p_2', p_2\right) | l, S, J; 1 \rangle \\
&= \int d^3q_1' d^3q_2' d^3q_1 d^3q_2 \sum \Bigg[\left\langle \begin{matrix} \frac{1}{2} & \frac{1}{2} \\ m_{S2} & m_{S3}' \end{matrix} \middle| \begin{matrix} 1 \\ m_{S23}' \end{matrix} \right\rangle \left\langle \begin{matrix} 1 & l_{p1}' \\ m_{S23}' & m_{p1}' \end{matrix} \middle| \begin{matrix} 1 \\ m_D' \end{matrix} \right\rangle \left\langle \begin{matrix} 1 & \frac{1}{2} \\ m_D' & m_{S1}' \end{matrix} \middle| \begin{matrix} S' \\ m_S' \end{matrix} \right\rangle \left\langle \begin{matrix} S' & l' \\ m_S' & m_l' \end{matrix} \middle| \begin{matrix} J \\ M \end{matrix} \right\rangle \\
&\times \left\langle \begin{matrix} \frac{1}{2} & \frac{1}{2} \\ m_{S3}' & m_{S1}' \end{matrix} \middle| \begin{matrix} S_n \\ m_{Sn}' \end{matrix} \right\rangle \left\langle \begin{matrix} S_n & L_n \\ m_{Sn}' & m_n' \end{matrix} \middle| \begin{matrix} j_n \\ m_{jn} \end{matrix} \right\rangle Y_{l',m_l'}^*(\hat{q}_1') \frac{\delta(q - q_1')}{q^2} Y_{l_{p1}',m_{p1}'}^*(\hat{p}_1') N \frac{u_{l_{p1}',1}^{0,1}(p_1')}{E_D - p_1'^2/m} Y_{L_n,m_n'}(\hat{p}_2') u_{L_n,j_n}^{I_n,S_n}(p_2') \Bigg] \\
&\times \delta^3(\vec{q}_2' - \vec{q}_2) \frac{\lambda_{L_n,j_n}^{I_n,S_n}}{g_{L_n,j_n}^{I_n,S_n}(W - 3q_2^2/4m)} (\text{same } [\ ], \text{ dropping the single primes}) \\
&\times \left\langle \begin{matrix} \frac{1}{2} & \frac{1}{2} \\ I_{z2} & I_{z3}' \end{matrix} \middle| \begin{matrix} 0 \\ 0 \end{matrix} \right\rangle \left\langle \begin{matrix} \frac{1}{2} & \frac{1}{2} \\ I_{z3}' & I_{z1} = -\frac{1}{2} \end{matrix} \middle| \begin{matrix} I_n \\ I_{zn} \end{matrix} \right\rangle \left\langle \begin{matrix} \frac{1}{2} & \frac{1}{2} \\ I_{z3} & I_{z1} = -\frac{1}{2} \end{matrix} \middle| \begin{matrix} I_n \\ I_{zn} \end{matrix} \right\rangle \left\langle \begin{matrix} \frac{1}{2} & \frac{1}{2} \\ I_{z2} & I_{z3} \end{matrix} \middle| \begin{matrix} 0 \\ 0 \end{matrix} \right\rangle,
\end{aligned} \tag{2.13}$$

where p_i is the relative momentum of particles j and k. In this equation we have made use of the fact that particle 2 is a spectator to an interaction in channel 2 so that $m_{S2}' = m_{S2}$, and $I_{z2}' = I_{z2}$. The sum is over all azimuthal components of angular momentum, spin, and isospin except, of course, M. In addition l_{p1} and l_{p1}' are each summed over the values 0 and 2 to give the central and tensor parts of the deuteron.

The isospin sum is trivial and gives $\frac{1}{4}(2I_n+1)$. Following Ahamdzadeh and Tjon[13] we expand $\delta^3(\vec{q}_2' - \vec{q}_2)$ in terms of spherical harmonics and the integrals become

$$\int d^3q_1' \cdots d^3q_2 - \int_0^\infty dq_2 q_2^{\,2} \frac{1}{g^{I_n, S_n}_{L_n', j_n}(W - 3q_2^{\,2}/4m)}$$

$$\times \sum_{L'' M_L''} \left[\sum_{J_1' M_1'} \frac{8\pi^2}{2J_1'+1} \left(\frac{2L''+1}{4\pi}\right)^{1/2} \left\langle \begin{matrix} l_{p1} & l' \\ m_{p1}' & m_l' \end{matrix} \middle| \begin{matrix} J_1' \\ M_1' \end{matrix} \right\rangle \left\langle \begin{matrix} L_n' & L'' \\ m_n' & M_L'' \end{matrix} \middle| \begin{matrix} J_1' \\ M_1' \end{matrix} \right\rangle g^{I_n, S_n, L_n, j_n}_{J_1', L'', l', l_{p1}'} \right]$$

$$\times \text{(same [ ], dropping single primes)}, \tag{2.14}$$

where

$$g^{I_n, S_n, L_n, j_n}_{J_1, L'', l, l_{p1}} = \sum_{\substack{N_1, \\ n_{p1}, n_{p2}, n_l}} (-)^{n_{p1}} \left\langle \begin{matrix} l_{p1} & l \\ n_{p1} & n_l \end{matrix} \middle| \begin{matrix} J_1 \\ N_1 \end{matrix} \right\rangle \left\langle \begin{matrix} L_n & L'' \\ n_{p2} & 0 \end{matrix} \middle| \begin{matrix} J_1 \\ N_1 \end{matrix} \right\rangle \int_{-1}^{+1} d\cos\theta_{q_1q_2}\, Y_{l_{p1}, n_{p1}}(\theta_{q_2p_1}, 0)$$

$$\times Y_{l, n_l}(\theta_{q_1q_2}, 0)\, Y_{L_n, n_{p2}}(\theta_{q_2p_2}, 0)\, \frac{u^{0,1}_{l_{p1}, 1}(p_1)\, u^{I_n, S_n}_{L_n, j_n}(p_2)}{E_D - p_1^{\,2}/m}, \tag{2.15}$$

and the angles and p_1, p_2 are given by

$$\cos\theta_{q_2p_2} = \frac{\frac{1}{2}q_2 + q\cos\theta_{q_2q_2}}{p_2}, \qquad \sin\theta_{q_2p_2} = \frac{q}{p_2}\sin\theta_{q_1q_2},$$

$$\cos\theta_{q_1p_1} = -\frac{q_2 + \frac{1}{2}q\cos\theta_{q_1q_2}}{p_1}, \qquad \sin\theta_{q_2p_1} = \frac{q}{2p_1}\sin\theta_{q_1q_2}, \tag{2.16}$$

$$p_1^{\,2} = \tfrac{1}{4}q^2 + q_2^{\,2} + q\,q_2\cos\theta_{q_1q_2}, \qquad p_2^{\,2} = q^2 + \tfrac{1}{4}q_2^{\,2} + q\,q_2\cos\theta_{q_1q_2}. \tag{2.17}$$

We now introduce into (2.13) and (2.14) the following sums over complete sets of states:

$$\Big\{ \sum_{S_{23}', S_{231}'} |[(\tfrac{1}{2}, \tfrac{1}{2})S_{23}', \tfrac{1}{2}]S_{231}', J_1'; J\rangle \langle [(\tfrac{1}{2}, \tfrac{1}{2})S_{23}', \tfrac{1}{2}]S_{231}', J_1'; J| \Big\} \text{ (same } \{\ \}\text{, dropping primes)}$$

$$\times \sum_{S''} |(j_n, \tfrac{1}{2})S'', L'', J\rangle \langle (j_n, \tfrac{1}{2})S'', L'', J|\,. \tag{2.18}$$

(The angular momentum coupling notation is similar to that used by Edmonds.[14]) The resulting set of 32 Clebsch-Gordan coefficients is then recognized as a product of four 12-j recouplings:

$$\text{C.G.} = \sum_{\substack{S'' \\ S_{231}' S_{231}}} \langle \{[(\tfrac{1}{2}, \tfrac{1}{2})S_{23} = 1, l_{p1}']S_D = 1, \tfrac{1}{2}\}S', l'; J | [(\tfrac{1}{2}, \tfrac{1}{2})S_{23} = 1, \tfrac{1}{2}]S_{231}', (l_{p1}', l')J_1'; J\rangle$$

$$\times \langle [(\tfrac{1}{2}, \tfrac{1}{2})S_{23} = 1, \tfrac{1}{2}]S_{231}', (L_n, L'')J_1'; J | \{[(\tfrac{1}{2}, \tfrac{1}{2})S_{31} = S_n, L_n]j_n, \tfrac{1}{2}\}S'', L''; J\rangle$$

$$\times \text{(same two recouplings, dropping single primes)}. \tag{2.19}$$

Using standard techniques the second 12-j recoupling may be reduced to a product of three 6-j symbols[14]:

$$\langle \{[(j_3, j_1)j_{31}, j_4]j_{314}, j_2\}j_{3142}, j_5; J | [(j_2, j_3)j_{23}, j_1]j_{231}, (j_4, j_5)j_{45}; J\rangle$$

$$= (-)^{j_1+j_2+j_3+j_5+j_{31}-j_{314}+J}[(2j_{23}+1)(2j_{31}+1)(2j_{45}+1)(2j_{231}+1)(2j_{314}+1)(2j_{3142}+1)]^{1/2}$$

$$\times \begin{Bmatrix} j_1 & j_3 & j_{31} \\ j_2 & j_{231} & j_{23} \end{Bmatrix} \begin{Bmatrix} j_4 & j_{31} & j_{314} \\ j_2 & j_{3142} & j_{231} \end{Bmatrix} \begin{Bmatrix} j_{231} & j_4 & j_{3124} \\ j_5 & J & j_{45} \end{Bmatrix}. \tag{2.20}$$

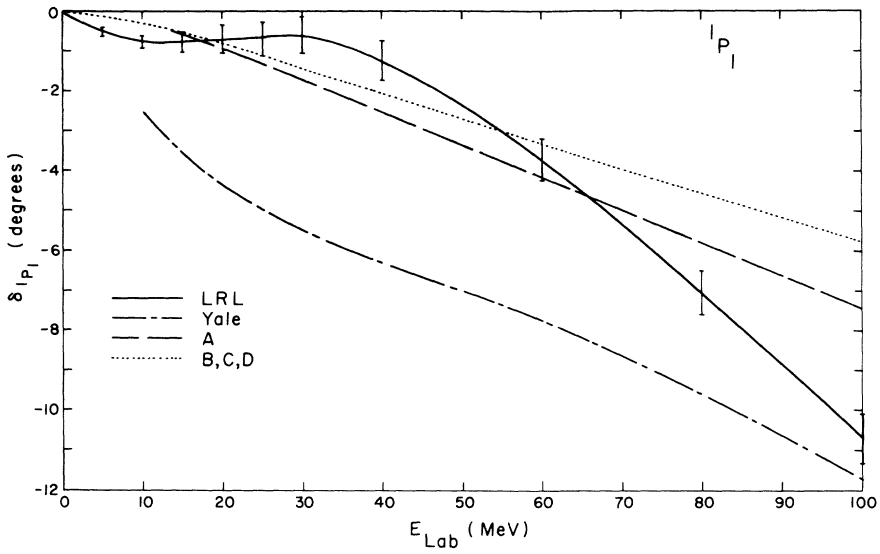

FIG. 4. $^1P_1$ phase shifts. The long-dashed line is Set A, while the dotted line is Sets B, C, and D.

Similarly, the first 12-j recoupling is a product of only two 6-j symbols, since the $(S_2, S_3)S_{23}$ coupling is the same in both sides. Thus (2.19) becomes

$$\text{C.G.} = 9(2S_n+1)(2j_n+1)(2J_1'+1)(2J+1)[(2S'+1)(2S+1)]^{1/2}$$

$$\times\sum_{S''}(2S''+1)\left[\sum_{S_{231}'}(2S_{231}'+1)\begin{Bmatrix}\frac{1}{2} & \frac{1}{2} & S_n\\ \frac{1}{2} & S_{231}' & 1\end{Bmatrix}\begin{Bmatrix}S_{231}' & l_{p1}' & S'\\ 1 & \frac{1}{2} & 1\end{Bmatrix}\begin{Bmatrix}S'' & L_n & S_{231}'\\ S_n & \frac{1}{2} & j_n\end{Bmatrix}\begin{Bmatrix}S_{231}' & l_{p1}' & S'\\ l' & J & J_1'\end{Bmatrix}\begin{Bmatrix}S_{231}' & L_n & S''\\ L'' & J & J_1'\end{Bmatrix}\right]$$

$$\times(\text{same }[\ ],\ \text{dropping single primes}). \tag{2.21}$$

The first 6-j symbol in (2.21) may be explicitly written out. Doing this and collecting all the pieces, we

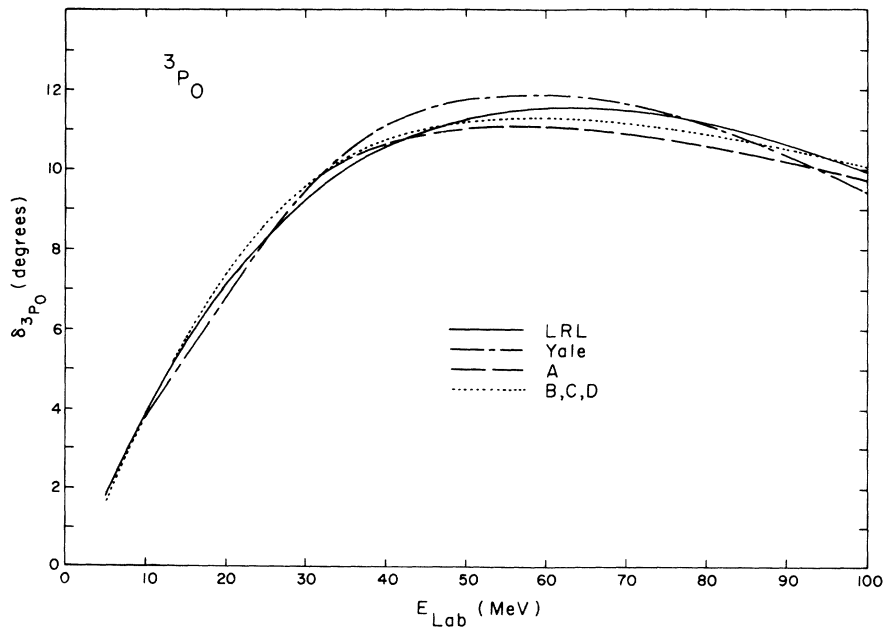

FIG. 5. $^3P_0$ phase shifts. The curves are as in Fig. 4.

have our final expression for (2.13):

$$\langle l', S', J; 1 | \bar{t}^{I_n, S_n}_{L_n, j_n}(2) | l, S, J; 1\rangle$$

$$= \tfrac{9}{4}\pi^3 N \lambda^{I_n, S_n}_{L_n, j_n} \frac{(2I_n+1)(2j_n+1)}{2S_n+1} [(2S'+1)(2S+1)]^{1/2} \int_0^\infty dq_2 \frac{{q_2}^2}{g^{I_n, S_n}_{L_n, j_n}(W - 3{q_2}^2/4m)}$$

$$\times \sum_{L''}(2L''+1) \sum_{S''}(2S''+1) \Bigg[\sum_{\substack{S'_{231}, J'_1, \\ l'_{p1}}} (-)^{S'_{231}-1/2}(2S'_{231}+1)^2 \begin{Bmatrix} S'_{231} & l'_{p1} & S' \\ 1 & \frac{1}{2} & 1 \end{Bmatrix} \begin{Bmatrix} S'' & L_n & S'_{231} \\ S_n & \frac{1}{2} & j_n \end{Bmatrix}$$

$$\times \begin{Bmatrix} S'_{231} & l'_{p1} & S' \\ l' & J & J'_1 \end{Bmatrix} \begin{Bmatrix} S'_{231} & L_n & S'' \\ L'' & J & J'_1 \end{Bmatrix} g^{I_n, S_n, L_n, j_n}_{J'_1, L'', l, l'_{p1}} \Bigg] (\text{same } [\ ], \text{ dropping single primes}), \tag{2.22}$$

where the integral g is defined in (2.15) and N is the deuteron normalization (2.12).

The sums on l'_{p1} and l_{p1} are over the values 0 and 2 corresponding to the central and tensor parts of the deuteron. The remaining sums are limited by the triangular rules in the 6-j symbols and the integral g. For the singlet forces ($S_n = 0$), (2.22) simplifies somewhat:

$$\langle l', S', J; 1 | \bar{t}^{I_n, S_n=0}_{L_n, j_n=L_n}(2) | l, S, J; 1\rangle$$

$$= (-)^{S+S'+1} 6\pi^3 N \lambda^{I_n, 0}_{L_n, L_n}(2I_n+1) \int_0^\infty dq_2 \frac{{q_2}^2}{g^{I_n, 0}_{L_n, L_n}(W - 3{q_2}^2/4m)}$$

$$\times \sum_{\substack{l'_{p1}, l_{p1}, \\ J_1}} (-)^{\frac{1}{2}(l'_{p1}+l_{p1})} \frac{1}{2J_1+1} \begin{Bmatrix} \frac{1}{2} & l'_{p1} & S' \\ l' & J & J_1 \end{Bmatrix} \begin{Bmatrix} \frac{1}{2} & l_{p1} & S \\ l & J & J_1 \end{Bmatrix} \sum_{L''}(2L''+1) g^{I_n, 0, L_n, L_n}_{J_1, L'', l', l'_{p1}} g^{I_n, 0, L_n, L_n}_{J_1, L'', l, l_{p1}}. \tag{2.23}$$

In actual computations it is advantageous to write out (2.22) and (2.23) as a sum of four terms corresponding to l'_{p1} and l_{p1} being 0 or 2. Then in all cases, except $l'_{p1} = l_{p1} = 2$, further simplification will be achieved due to a zero in a 6-j symbol. It should be noted that since (2.22) and (2.23) are not written for the force in the $I_n = 0$, $S_n = j_n = 1$ channel, the two-nucleon T matrix does not have a bound-state pole, and hence the bar on $\bar{t}$ is redundant.

We will now write down the expression analogous to (2.22) for the force binding the deuteron. In this case there will be 16 terms corresponding to having a central or tensor term in the bra or ket and in either "side" of the separable T matrix. The methods for evaluating the angular integrals and the spin sums are the same as used above:

$$\langle l', S', J; 1 | \bar{t}^{I_n=0, S_n=1}_{j_n=1}(2) | l, S, J; 1\rangle$$

$$= \tfrac{9}{4}\pi^3 N [(2S+1)(2S'+1)]^{1/2} \lambda^{0,1}_1 \sum_{L'', S''}(2L''+1)(2S''+1) \mathrm{P} \int_0^\infty dq_2 \frac{{q_2}^2}{g^{0,1}_1(W - 3{q_2}^2/4m)}$$

$$\times \Bigg[\sum_{\substack{l'_{p1}, l'_{p2}, \\ J'_1, S'_{231}}} (-)^{S'_{231}-1/2}(2S'_{231}+1)^2 \begin{Bmatrix} S'_{231} & l'_{p1} & S' \\ 1 & \frac{1}{2} & 1 \end{Bmatrix} \begin{Bmatrix} S'_{231} & l'_{p2} & S'' \\ 1 & \frac{1}{2} & 1 \end{Bmatrix} \begin{Bmatrix} S'_{231} & l'_{p1} & S' \\ l' & J & J'_1 \end{Bmatrix} \begin{Bmatrix} S'_{231} & l'_{p2} & S'' \\ L'' & J & J'_1 \end{Bmatrix} g^{0,1,l'_{p2},1}_{J'_1, L'', l', l'_{p1}} \Bigg]$$

$$\times (\text{same } [\ ], \text{ dropping single primes}). \tag{2.24}$$

Here the integral on dq_2 is, as noted, a principal-value integral; if the full single-scattering term from the Faddeev equations[9] were desired, one would simply add the $-i\pi\delta(q_2 - q)$ term corresponding to using a $+i\epsilon$ prescription at the zero of $g^{0,1}_1$.

Since the Hamiltonian operator can be expressed in the same coordinates as the ket vector, the $\langle 2 | (W - H_0) | 1\rangle$ term of (2.3) is easily evaluated:

$$\langle l', S', J; 2 | (W - H_0) | l, S, J; 1\rangle = \langle l', S', J; 2 | V^{I_n=0, S_n=1}_{j_n=1}(1) | l, S, J; 1\rangle$$

$$= \tfrac{3}{2}\pi^{3/2} N [(2l'+1)(2S'+1)(2S+1)]^{1/2} \sum_{\substack{l_{p2}, l_{p1}, \\ J_1, S_{231}}} (-)^{S_{231}-1/2}(2S_{231}+1)^2$$

$$\times \begin{Bmatrix} S_{231} & l_{p2} & S' \\ 1 & \frac{1}{2} & 1 \end{Bmatrix} \begin{Bmatrix} S_{231} & l_{p1} & S \\ 1 & \frac{1}{2} & 1 \end{Bmatrix} \begin{Bmatrix} S_{231} & l_{p2} & S' \\ l' & J & J_1 \end{Bmatrix} \begin{Bmatrix} S_{231} & l_{p1} & S \\ l & J & J_1 \end{Bmatrix} g^{0,1,l_{p2},1}_{J_1, l', l, l_{p1}}. \tag{2.25}$$

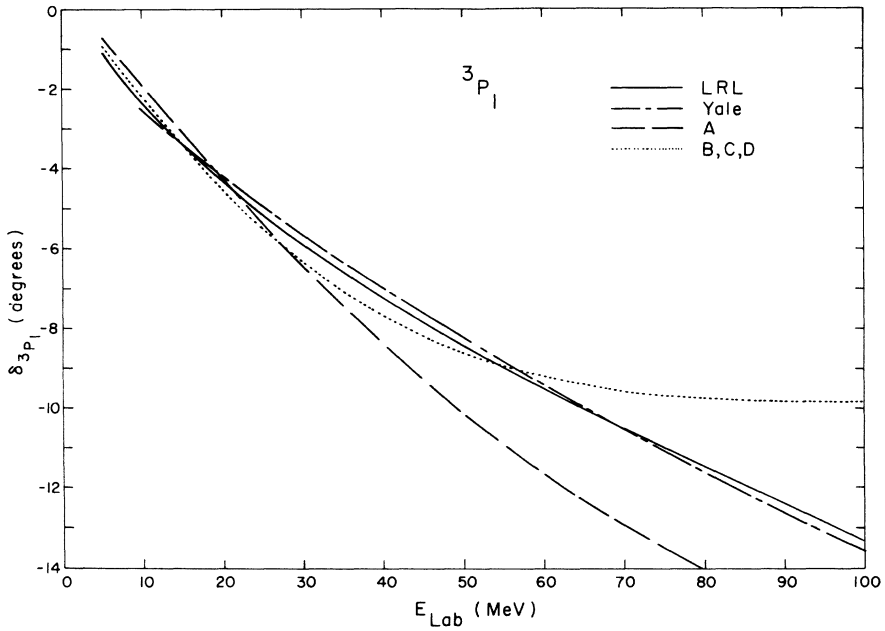

FIG. 6. $^3P_1$ phase shifts. The curves are as in Fig. 4.

We complete our evaluation of the matrix elements in (2.3) with the observation[4] that for separable potentials

$$\langle l', S', J; 3 | \bar{t}_2 | l, S, J; 1\rangle = \langle l', S', J; 1 | \bar{t}_2 | l, S, J, 1\rangle . \tag{2.26}$$

Also time-reversal invariance tells us that[8]

$$\bar{U}^J(l', S' | l, S) = \bar{U}^J(l, S | l', S') , \tag{2.27}$$

which reduces the number of terms we have to evaluate.

Equations (2.22)–(2.27) with (2.16) reduce the computation of the $\bar{U}^J(l', S' | l, S)$ amplitudes to a sum of two-dimensional integrals which are done numerically. In doing these integrals it is important to take note of the singularities of the integrand. The integral over q_2 is broken into two regions such that the parametric energy is positive in one ($0 \leq q_2{}^2 \leq \frac{4}{3}mW$) and negative in the other ($\frac{4}{3}mW \leq q_2{}^2$). In the former, $g(W - \frac{4}{3}mq_2{}^2)$ is complex and its imaginary piece has a square-root singularity (in terms of q_2) at the upper point of

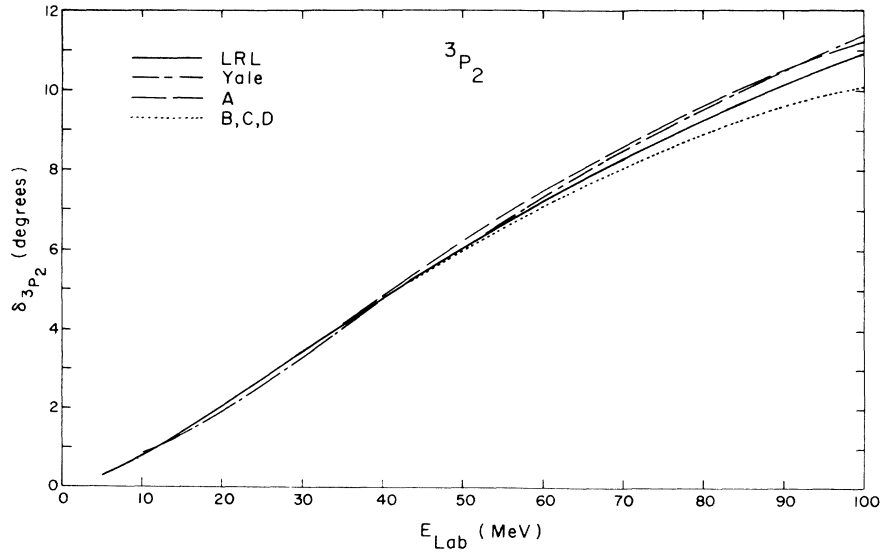

FIG. 7. $^3P_2$ phase shifts. The curves are as in Fig. 4.

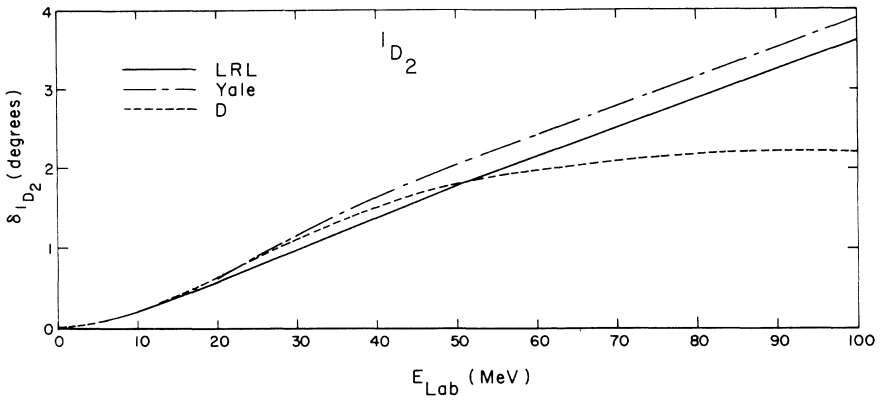

FIG. 8. $^1D_2$ phase shifts. The dashed line is potential Set D. This phase shift is zero for the other four sets.

this region. [g is the only complex quantity entering the $\overline{U}$ amplitudes; if it is the last quantity to be multiplied into (2.22)–(2.24), all the rest of the calculation is real arithmetic.] Similarly, the real part of g has a square-root singularity at the beginning of the second region. Transformations of variables should be used in each region to remove these singularities. The q_2 integral from $q_0=(\frac{4}{3}mW)^{1/2}$ to infinity is done by the transformation

$$q_2=\frac{2q_0+1+x}{1-x}; \quad -1\leq x\leq 1, \quad q_0\leq q_2\leq\infty,$$

where the points on $(-1, 1)$ have already been transformed to remove the square-root singularity noted above. In this way we avoid having to introduce a cutoff in q_2.

The principal value is handled by noting that

$$\mathrm{P}\int_0^\infty \frac{dq}{q^2-q_B^{\,2}}=0, \quad q_B^{\,2}=\tfrac{4}{3}m(W-E_D),$$

so that

$$\mathrm{P}\int_0^\infty \frac{f(q)dq}{q^2-q_B^{\,2}}=\int_0^\infty \frac{f(q)-f(q_B)}{q^2-q_B^{\,2}}dq$$

and the last integrand has no singularity at $q=q_B$.

The above analysis has been somewhat lengthy and implementing equations (2.22)–(2.25) on a computer involves a fair amount of work, especially if one works out all the special cases for

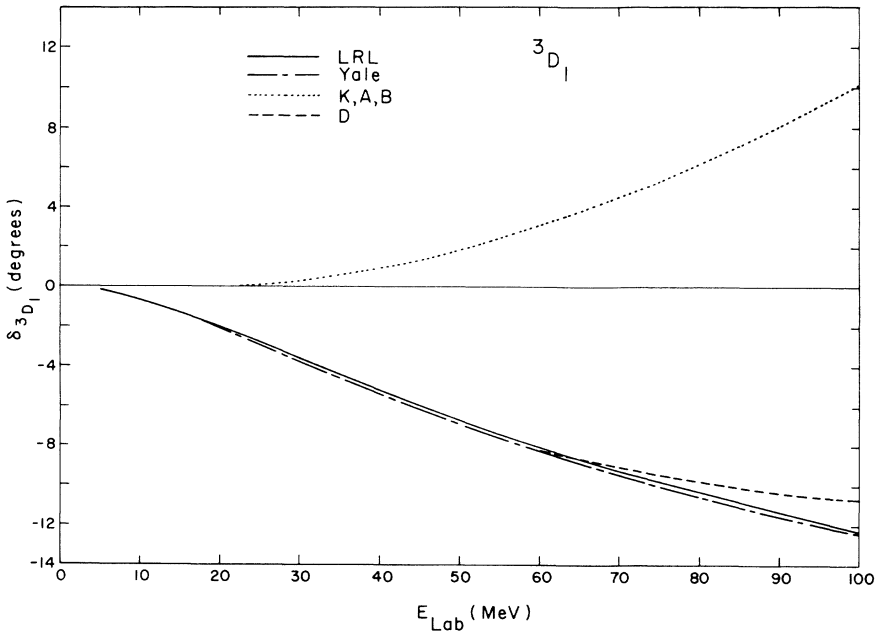

FIG. 9. $^3D_1$ phase shifts. The dotted line is potential Sets A, B, and K; the dashed line is Set D. For Set C this phase shift is zero. From 0. to 17. MeV the dashed curve (A, B, K) is negative with a minimum of −0.044° at 10 MeV.

l_{p1}, l_{p2}, etc., equal to 0 or 2. However, the resulting savings in computer time completely justify this effort; we estimate that such a program will run at least 1000 times faster than one in which the five-dimensional integral and all the sums in (2.13) are done numerically.[2] Calculations for S- and P-wave interactions using a maximum J of $\frac{19}{2}$ and a grid of 20×32 Gaussian points take about 50 sec of Univac 1108 time.

III. TWO-NUCLEON INPUT AND RESULTS

A. N-N Form Factors and Phase Shifts

We choose simple generalizations of the Yamaguchi[7] potentials for the form factors in (2.5) and (2.7). For the central potentials we use

$$u^{I;S}_{l,j}(p) = p^l[p^2+(\gamma^{I;S}_{l,j})^2]^{-l/2-1}. \tag{3.1}$$

For this form factor the integral in $g^{I;S}_{l,j}$ is straightforwardly evaluated in a recursive manner. The deuteron form factors were the same as used by Yamaguchi:

$$u^{0,1}_{0,1}(p) = \frac{1}{p^2+\gamma_c^{\,2}},$$
$$u^{0,1}_{2,1}(p) = \frac{rp^2}{(p^2+\gamma_t^{\,2})^2}, \tag{3.2}$$

where r is a parameter that determines the percent D state of the deuteron. For this form, (2.10) is[7]

$$g^{0,1}_1\left(W-\frac{3q^2}{4m}\right) = -[q^2-\tfrac{4}{3}m(W-E_D)]\frac{3m\pi\lambda}{16}$$
$$\times\left[\frac{\kappa+\kappa_0+2\gamma_c}{\gamma_c(\gamma_c+\kappa)^2(\gamma_c+\kappa_0)^2(\kappa+\kappa_0)}+\frac{r^2}{8}\frac{\gamma_t^{\,4}+4\gamma_t^{\,3}(\kappa+\kappa_0)+\gamma_t^{\,2}(\kappa^2+16\kappa\kappa_0+\kappa_0^{\,2})+5\kappa_0^{\,2}\kappa^2+4\gamma_t\kappa\kappa_0(\kappa^2+6\kappa\kappa_0+\kappa_0^{\,2})/(\kappa+\kappa_0)}{\gamma_t(\gamma_t+\kappa)^4(\gamma_t+\kappa_0)^4}\right], \tag{3.3}$$

where

$$\kappa_0=(-mE_D)^{1/2}, \quad E_D<0,$$
$$\kappa=(-mE)^{1/2}=(\tfrac{3}{4}q^2-mW)^{1/2}=ip.$$

Equation (3.3) explicitly displays the deuteron pole for the principal-value integral in (2.24). Formulas for the properties of the deuteron bound state for the potential (3.2) may be found in Ref. 7.[15]

Five sets of potentials were used in the calculations. The N-N partial-wave content of these sets and the actual parameters used are given in Table I. The two-nucleon scattering phase shifts of these potentials for laboratory energies less than 100 MeV are given in Figs. 1–11,[16–18] while differential cross sections and polarizations at 40 MeV are given in Figs. 12 and 13.[19] The Yale[16] and Livermore[17] phase shifts are also shown. In general the rank-one separable potentials give an adequate representation of the low-energy data. The obvious exception is the ϵ_1 and $\delta_{^3D_1}$ curves for the $^3S_1$-$^3D_1$ tensor force (designation 3ST). The reason for this failure is clear: A rank-one $^3S_1$-$^3D_1$ separable potential requires $t^{0,1}_{0,0,1}$, $t^{0,1}_{2,0,1}$, $t^{0,1}_{0,2,1}$, and $t^{0,1}_{2,2,1}$ (the notation is $t^{I;S}_{l',l,j}$) to all have the same phase. Since this is experimentally not the case, higher-rank potentials will be needed to represent these coupled channels. It was because of this failure of the tensor force that we included potential Sets C and D which contain an S-wave deuteron (D-state probability = 0). Note that in Set D, since no mixing force is provided, the $^3D_1$ channel is independent of the $^3S_1$ channel. The potential Set K is the same as the potentials used in KK. It should also be noted that since all the $S=1$ amplitudes have the same phase for the Yamaguchi tensor potentials, the two-nucleon (n-p and n-n) polarizations for Set K are identically zero.[20]

B. N-d Cross Sections and Polarizations

Table II shows a few of the unitarized elastic N-d amplitudes for Set K at 22.7 MeV. These were computed with 32 Gaussian points in the q_2 integral and 20 points in the $\cos\theta_{q_1q_2}$ integrals and are stable to five places. Cross sections and polarizations generated from the Table II amplitudes are in agreement with recent results of Aarons and Sloan.[5] In Table III we show the convergence of $d\sigma/d\Omega$ and the polarization at 22.7 MeV as more angular momentum states are added. It is clear from these results that a large number of partial-wave amplitudes must be used to achieve reliable results, especially in the backwards direction.[5] In the results that follow we truncated the sum on J at $\frac{19}{2}$, for which $d\sigma/d\Omega$ and polarizations (with the exception of polarizations for Set K) have converged to better than 1% (i.e., two significant figures). Aarons and Sloan have noted that truncation on l' and l instead of J will produce more rapid convergence of the polarization.[5]

Figures 14–19[21–27] show the elastic N-d cross sections and polarizations at 14.1-, 22.7-, and 40.0-MeV laboratory energy. In the $d\sigma/d\Omega$ graphs we have not drawn all five potential sets, since

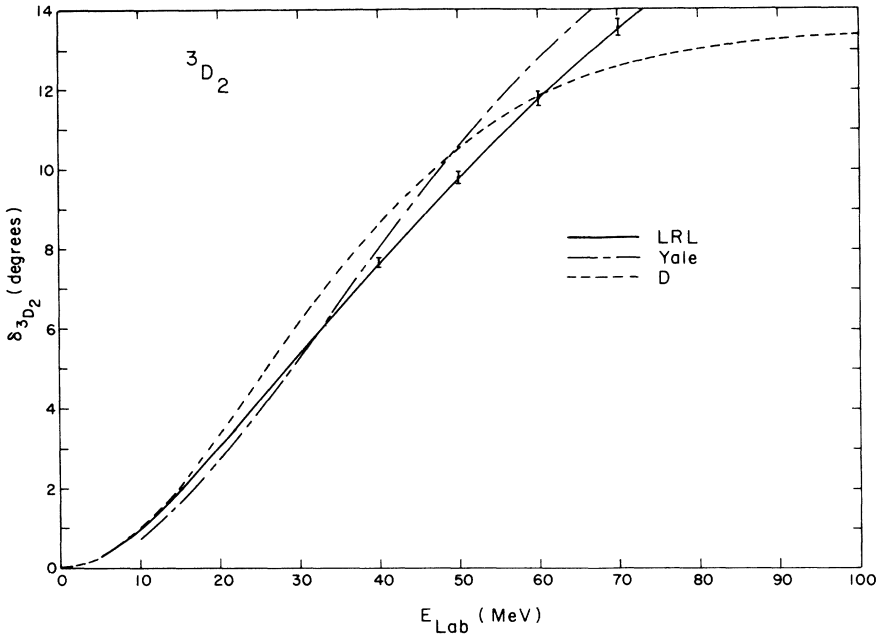

FIG. 10. $^3D_2$ phase shifts. The curves are as in Fig. 8.

the curves overlap a great deal.

The curves labeled K are for the potential used in KK. As noted by Aarons and Sloan[5] these curves disagree with those of KK and, furthermore, the discrepancy is not entirely due to the low angular momentum truncation used in KK. Since the present graphs are in agreement with those of Aarons and Sloan we conclude that the results of KK are erroneous.[6]

Two conclusions can be drawn from Figs. 14–19. First, the Sloan approximation does not seem capable of explaining the polarization in N-d scattering at low energies.[28] Unlike Set K, potentials A–D yield N-d polarizations of magnitude comparable to the experimentally measured results. However, although curves A through D represent a fair variety of N-N potentials, all fail to fit the experimental polarizations even qualitatively with the possible exception of the extreme forward direction. We do not believe that this failure is due to the poor properties mentioned earlier of the rank-one $^3S_1$-$^3D_1$ potential for the following reasons. The only difference between B and C is that in C the tensor part of this force is set to zero so that $\epsilon_1 = \delta_{^3D_1} = 0$. (The $^3S_1$ phase shifts differ by less than 1% up to 10 MeV and by less than 7% up to 100 MeV.) In D a good representation of the D-wave phase shifts is added to C (still keeping $\epsilon_1 = 0$.) Although the polarization curves for Set D have slight qualitative differences from B, it does not seem reasonable, in view of the small difference between B and C, to assume that the inclusion of a good mixing term will force curve D into agreement with the data (remember that the ϵ_1 term removed in going from B to C had a magnitude of some 10 times greater than the phase-shift analyses). It is interesting to note that the structure of these polarization curves at

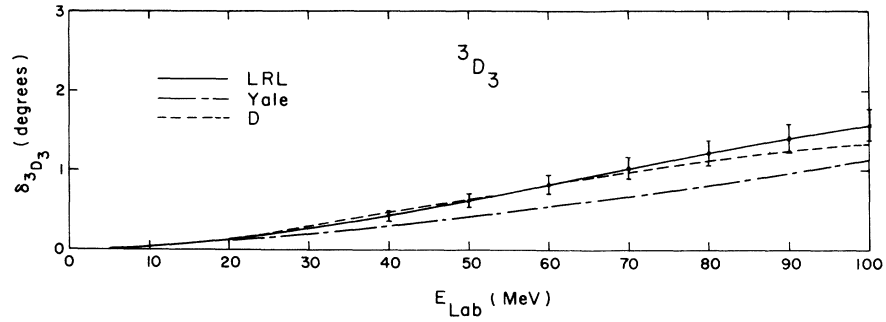

FIG. 11. $^3D_3$ phase shifts. The curves are as in Fig. 8.

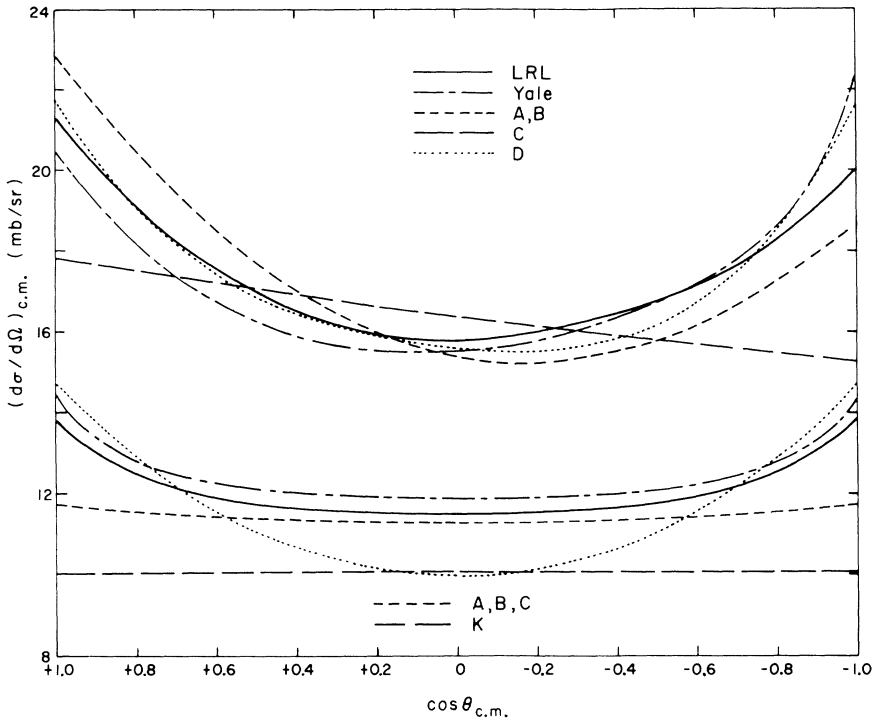

FIG. 12. Two-nucleon differential cross sections at 40-MeV laboratory energy. The upper set of curves is n-p scattering, the lower set is n-n scattering. The Livermore VII, IX values are given by the solid line, and the Yale Y-IV values are given by the dash-dot line. In the upper set, the short-dashed line is A and B; the long-dashed line is C; K is not shown. In the lower set the short dash line is A, B, C; the long dash is K. In both sets the dotted line is D.

TABLE II. Values of the N-d partial-wave amplitudes at 22.7 MeV for potential Set K. The amplitudes are normalized so that $\sigma^J(l', S'|l, S) = 4\pi |f^J(l', S'|l, S)|^2/q^2$.

J^P	l'	S'	$f^J(l', S'\|l, S)$		
			$l, S=0, \frac{1}{2}$	$l, S=2, \frac{3}{2}$	
$\frac{1}{2}^+$	0	$\frac{1}{2}$	$0.195\,51+0.772\,38i$	$-0.021\,448-0.028\,840i$	
	2	$\frac{3}{2}$	$-0.021\,448-0.028\,840i$	$-0.101\,99+0.055\,052i$	
			$l, S=1, \frac{1}{2}$	$l, S=1, \frac{3}{2}$	
$\frac{1}{2}^-$	1	$\frac{1}{2}$	$0.077\,229+0.227\,87i$	$-0.039\,397-0.052\,822i$	
	1	$\frac{3}{2}$	$-0.039\,397-0.052\,822i$	$0.224\,30+0.158\,02i$	
			$l, S=0, \frac{3}{2}$	$l, S=2, \frac{1}{2}$	$l, S=2, \frac{3}{2}$
$\frac{3}{2}^+$	0	$\frac{3}{2}$	$-0.113\,35+0.438\,85i$	$-0.280\,03\times10^{-1}+0.151\,98\times10^{-1}i$	$0.657\,78\times10^{-2}-0.609\,65\times10^{-1}i$
	2	$\frac{1}{2}$	$-0.280\,03\times10^{-1}+0.151\,98\times10^{-1}i$	$0.108\,65+0.636\,73\times10^{-1}i$	$-0.388\,28\times10^{-2}-0.860\,06\times10^{-2}i$
	2	$\frac{3}{2}$	$+0.657\,78\times10^{-2}-0.609\,65\times10^{-1}i$	$-0.388\,28\times10^{-2}-0.860\,06\times10^{-2}i$	$0.109\,96+0.424\,40\times10^{-1}i$
			$l, S=1, \frac{1}{2}$	$l, S=1, \frac{3}{2}$	$l, S=3, \frac{3}{2}$
$\frac{3}{2}^-$	1	$\frac{1}{2}$	$0.788\,97\times10^{-1}+0.231\,20i$	$0.152\,35\times10^{-1}+0.209\,82\times10^{-1}i$	$0.388\,53\times10^{-1}-0.270\,14\times10^{-3}i$
	1	$\frac{3}{2}$	$0.152\,35\times10^{-1}+0.209\,82\times10^{-1}i$	$0.317\,14+0.270\,15i$	$-0.123\,06\times10^{-1}-0.137\,40\times10^{-1}i$
	3	$\frac{3}{2}$	$0.388\,53\times10^{-1}-0.270\,14\times10^{-3}i$	$-0.123\,06\times10^{-1}-0.137\,40\times10^{-1}i$	$0.469\,25\times10^{-1}+0.127\,02\times10^{-1}i$

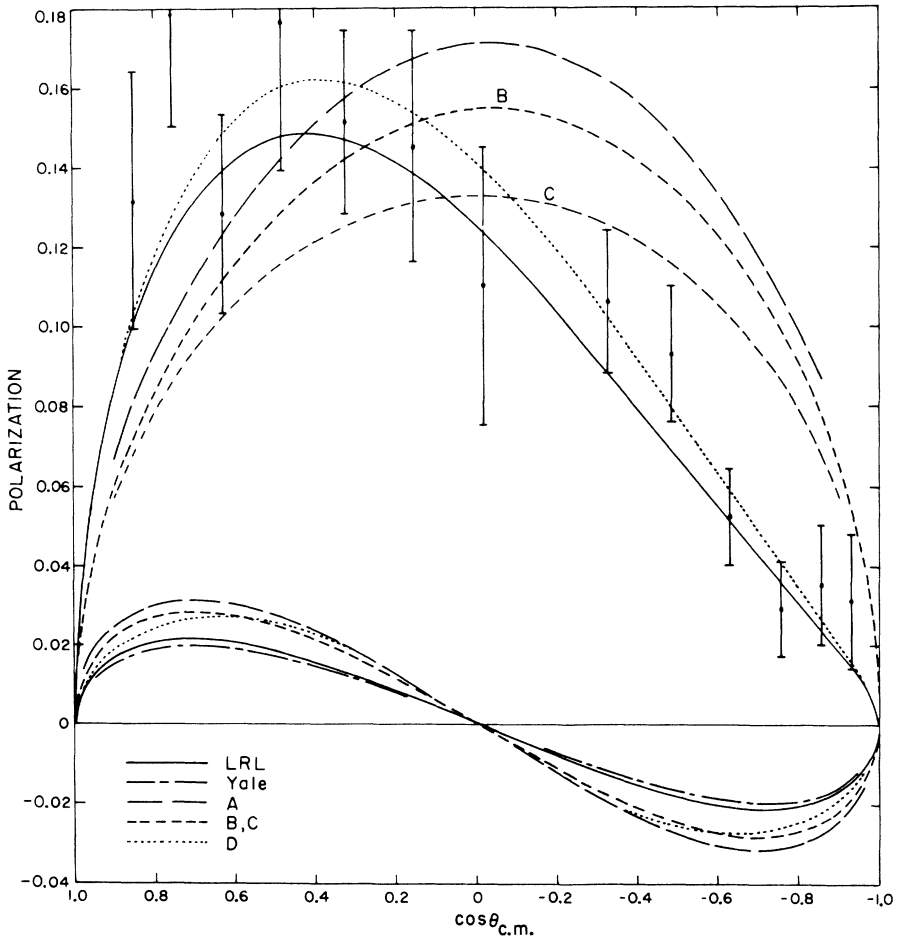

FIG. 13. Two-nucleon polarizations at 40 MeV. The upper set of curves is for n-p scattering; the lower set is n-n scattering. For n-p both the Yale and Livermore analyses give the same polarization as shown by the solid line. The error bars are data by Langsford *et al.* (Ref. 19). The long dash is Set A; short dash is B and C; dotted line is Set D. Set K gives zero N-N polarization.

TABLE III. Convergence of the N-d cross section and polarization at 22.7 MeV.

	$d\sigma/\Omega$ for potential Set K (mb/sr)			Polarization at $\theta = 90°$	
J_{max}	$\theta = 0°$	$\theta = 90°$	$\theta = 180°$	Set K	Set C
$\frac{1}{2}$	7.91	5.43	2.94	+0.0272	+0.00547
$\frac{3}{2}$	31.7	7.82	9.46	−0.259	−0.154
$\frac{5}{2}$	53.3	5.46	33.0	+0.113	+0.320
$\frac{7}{2}$	56.5	5.10	53.1	+0.0935	0.245
$\frac{9}{2}$	58.8	4.98	65.7	−0.0112	0.153
$\frac{11}{2}$	58.6	4.94	72.2	−0.00589	0.170
$\frac{13}{2}$	59.0	4.96	75.4	+0.0154	0.187
$\frac{15}{2}$	58.9	4.96	76.9	+0.0141	0.184
$\frac{17}{2}$	58.9	4.96	77.6	+0.0100	0.181
$\frac{19}{2}$	58.9	4.96	77.9	+0.0103	+0.182
$\frac{21}{2}$	58.9	4.96	78.0	+0.0111	

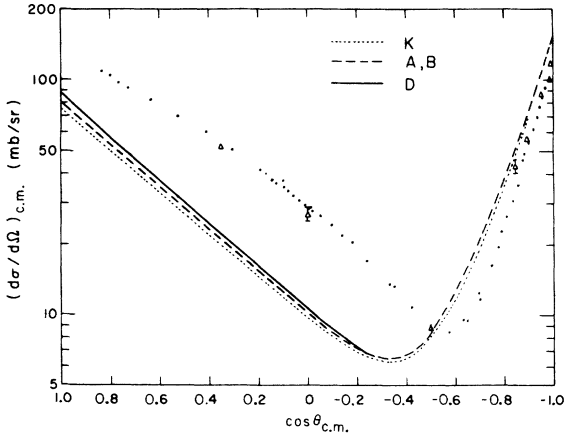

FIG. 14. N-d differential cross sections at 14.1-MeV lab energy. The dotted line is Set K; the dashed line is Sets A and B; the solid line is Set D. Set C lies between Sets A, B and Set D. The data are from Kikuchi *et al.* (Ref. 21) (13.93 MeV) (dots) and Seagrave (Ref. 22) (triangles).

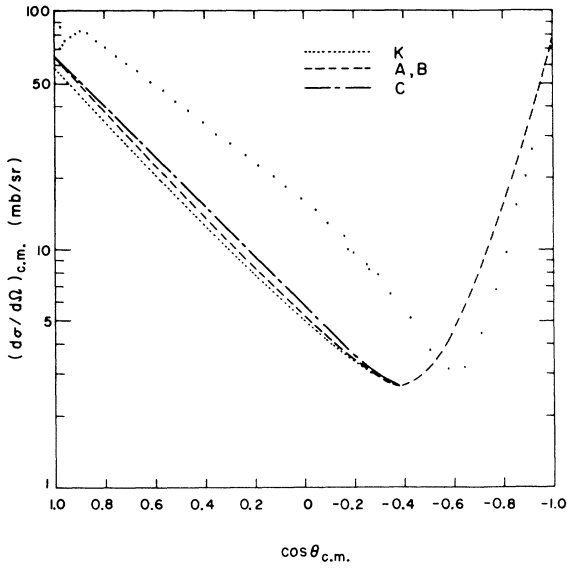

FIG. 15. *N-d* differential cross sections at 22.7 MeV. The dotted line is Set K; the dashed line is Sets A and B; the dash-dot line is Set C. Set D was not computed at this energy. The data are from Bunker *et al.* (Ref. 23) (22.0 MeV).

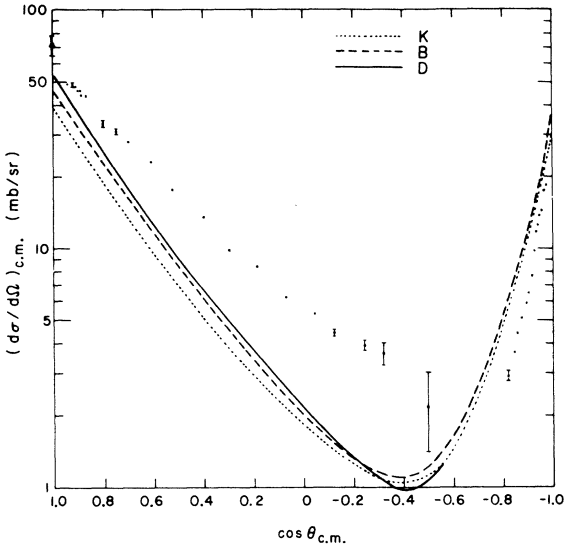

FIG. 16. *N-d* differential cross sections at 40.0 MeV. The dotted line is Set K; the dashed line is Set B and the solid line is Set D. Set A lies close to B, while Set C lies close to D. The data are from Williams and Brussel (Ref. 24); the triangle is Holdeman and Thaler's (Ref. 25) extrapolation of this data to the forward direction.

40 MeV is approximately the same as that obtained using an on-shell form of the impulse approximation with the exchange term included.[29]

Similarly the Sloan approximation does not seem capable of yielding the magnitude of the forward diffraction peak.[28,30] At 14.1 MeV, curve D is almost 50 mb beneath the extrapolated experimental forward cross section, while the difference between curves K and D is only 16 mb. It seems doubtful that the addition of higher partial waves in the nucleon-nucleon channel will make up the remaining 50 mb. Although the discrepancy at 40 MeV is not so great it appears to be due to the Sloan approximation as opposed to the potentials used. We have made several calculations using the single scattering form of the fixed-scatterer

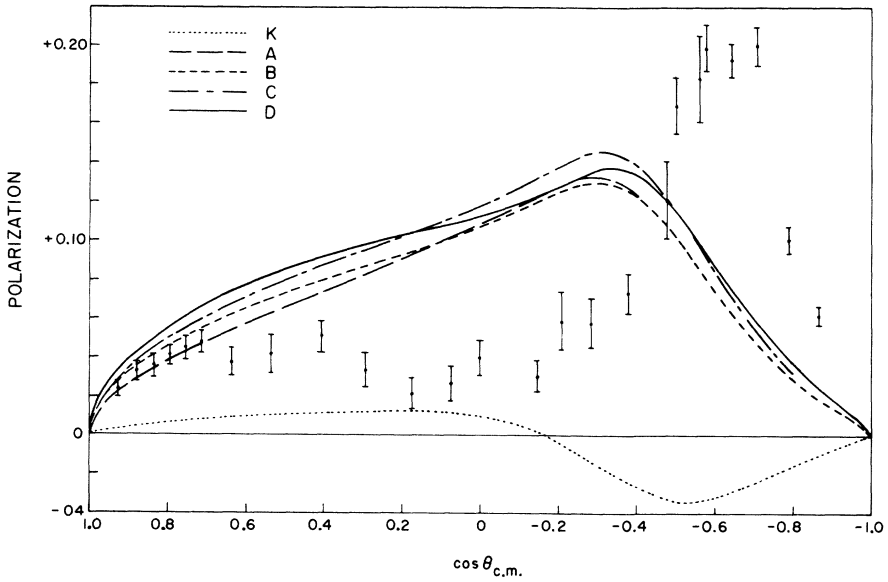

FIG. 17. *N-d* polarization at 14.1 MeV. The dotted line is Set K; the long dash is Set A; the short dash is Set B; the dash-dot is Set C; and the solid line is Set D. The data are from Faivre *et al.* (Ref. 26) (14.5 MeV).

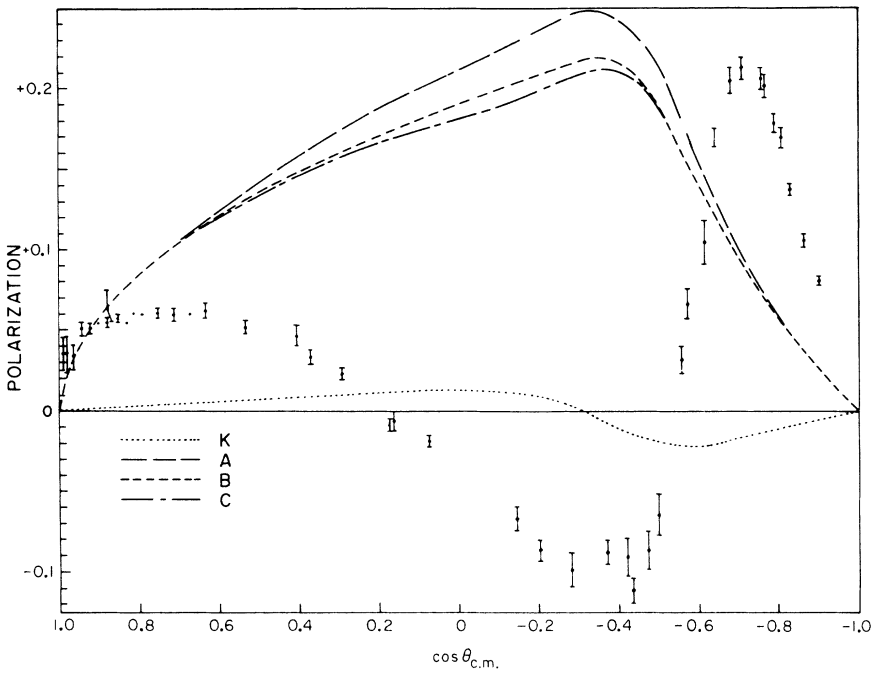

FIG. 18. N-d polarization at 22.7 MeV. The curves are as in Fig. 17, except D is not shown. The data are from Faivre *et al.* (Ref. 26).

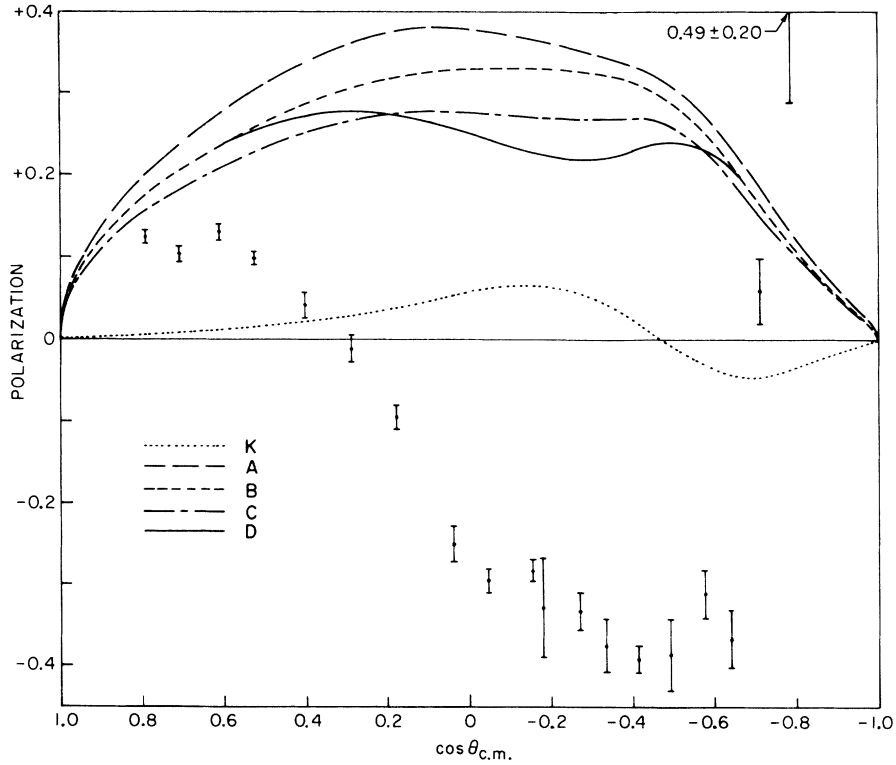

FIG. 19. N-d polarization at 40.0 MeV. The curves are as in Fig. 17. The data are from Conzett *et al.* (Ref. 27).

approximation[31] employing the potentials K, A–D, as well as the complete set of Livermore phase shifts. The values of the forward $d\sigma/d\Omega$ at 40 MeV range from slightly too low (63. mb/sr) for Set K, to good agreement (77. mb/sr) for Set B, to a slightly too large value (83.7 mb/sr) for the Livermore phases. Thus, the potentials used here with the possible exception of Set K should be adequate to predict the approximate value of the forward cross sections.

The other conclusion is that any attempt to explain the polarization in N-d scattering, either via "exact" or approximate three-body calculation, must include P-wave two-nucleon amplitudes. Despite our poor results, comparison of curves K and A or B indicates that the P-wave forces make a very large contribution to the N-d polarization. We have also made fixed-scatterer[31] and nonunitarized Faddeev-type impulse calculations [the latter consists of leaving the δ-function part of the deuteron pole in (2.3) and directly equating the three-body T matrix with the $\bar{U}$ amplitudes] for the various potential sets. The results are similar to the unitary-model results: For Set K the N-d polarizations are always very small; while for Sets A–D they have magnitudes comparable to experiment and structure similar to curves A–D in Figs. 17–19. Thus, including just the tensor component in the deuteron is not adequate to explain N-d polarization; indeed, curves B and C suggest that it is not necessary and represents only a small correction. This conclusion is substantiated by the results of Kottler and Kowalski,[29] who found small effects from the D-wave part of the deuteron at 40 MeV in an on-shell impulse calculation. However, at 150 MeV the tensor component was important to giving a good fit to the data.

A final comment is called for concerning the appropriateness of the potentials employed here. Although our rank-one separable potentials have fairly good phase shifts, it could perhaps be objected that their off-shell behavior may be pathological. This could be important, since in the impulse matrix elements the integral on q_2 runs over all negative two-body energies. Since we have not devised a potential with on-shell behavior similar to ours but radically different off-shell behavior, the only argument that we can offer against such an objection is that our results for the polarization are similar to those obtained from fixed-scatterer calculations that only use on-shell matrix elements. Thus it is doubtful that the off-shell behavior of our potentials is grossly distorting our results.[32]

IV. CONCLUSIONS

It appears that the Sloan approximation is not capable of predicting the rich polarization structure present in moderately-low-energy elastic N-d scattering. To a lesser extent the magnitude of the forward diffraction peak is not reproduced. By using increasingly sophisticated representations of the two-nucleon interaction it appears that the source of this failure lies in the approximation itself and is not the inadequacy of the N-N input.

The strong dependence of the N-d polarization on the presence of the P-wave channels of the N-N forces using the Sloan and other approximations indicates the necessity of including these potentials in future calculations (exact or otherwise) that attempt to predict the N-d polarization even at relatively low energies. In this regard the P-wave forces appear to be substantially more important than the tensor component of the $S = J = 1$ two-nucleon interaction. This result is somewhat discouraging, since the incorporation of the four P-wave channels will greatly complicate an "exact" calculation even when this is attempted using separable potentials.[33,34]

ACKNOWLEDGMENT

We are indebted to Professor Sloan and Dr. Aarons for the communication of their results prior to publication. We also wish to thank Professor Sloan for clarifying a point on the singularities of the integrand.

---

*Work supported in part by the U. S. Atomic Energy Commission.

[1]J. Krauss and K. L. Kowalski, Phys. Letters 31B, 263 (1970).

[2]J. Krauss and K. L. Kowalski, Phys. Rev. C 2, 1319 (1970). References 1 and 2 will be collectively referred to as KK.

[3]The formalism and the main approximations introduced are due to Sloan (Ref. 4) who refers to this as the unitary first-order approximation. In this paper we will simply refer to this as the unitary model or, alternatively, as the Sloan approximation (cf. Refs. 1 and 2).

[4]I. H. Sloan, Phys. Rev. 165, 1587 (1968); 185, 1361 (1969).

[5]J. C. Aarons and I. H. Sloan, several private communications; and Phys. Rev. C 5, 582 (1972).

[6]The nature of the fortuitous error(s) in the computations reported in KK remains unknown despite several

attempts by the present authors to reproduce these results via various contrived errors. Unfortunately, our efforts in this regard were limited in that the original computer program utilized in KK was not available to us in the course of this research.

[7]Y. Yamaguchi and Y. Yamaguchi, Phys. Rev. 95, 1635 (1954).

[8]I. H. Sloan, Nucl. Phys. A139, 337 (1969).

[9]L. D. Faddeev, Zh. Eksperim. i Teor. Fiz. 39, 1459 (1960) [transl.: Soviet Phys.– JETP 12, 1014 (1961)].

[10]C. Lovelace, Phys. Rev. 135, B1225 (1964).

[11]R. T. Sharp and H. von Baeyer, J. Math. Phys. 7, 1105 (1966).

[12]J. M. Blatt and V. F. Weisskopf, *Theoretical Nuclear Physics* (Wiley, New York, 1952), Appendix A.

[13]A. Ahmadzadeh and J. A. Tjon, Phys. Rev. 139, B1085 (1965). As noted in R. Balian and E. Brézin, Nuovo Cimento 61B, 403 (1969), Eqs. (2.12) and (2.13) of this reference are missing a factor $(-1)^{M_L}$.

[14]A. R. Edmonds, *Angular Momentum in Quantum Mechanics* (Princeton U. P., Princeton, N. J., 1957). We use Edmonds's phase and normalizations for the 6-j symbols.

[15]The factor $1/[(\beta+\gamma)^2(\alpha+\gamma)^5]$ in the first line of Eq. (26) of Ref. 7 should read $1/[\alpha(\beta+\gamma)^2(\alpha+\gamma)^5]$.

[16]R. E. Seamon, K. A. Friedman, G. Breit, R. D. Haracz, J. M. Holt, and A. Prakash, Phys. Rev. 165, 1579 (1968). For the isotriplet phases we used the n-p scattering fit (Table III).

[17]M. H. MacGregor, R. A. Arndt, and R. M. Wright, Phys. Rev. 169, 1128 (1968); 173, 1272 (1968).

[18]H. P. Stapp, T. Ypsilantis, and N. Metropolis, Phys. Rev. 105, 302 (1957).

[19]A. Langsford, P. H. Bowen, G. C. Cox, G. B. Huxtable, and R. A. J. Riddle, Nucl. Phys. 74, 241 (1965).

[20]To our knowledge this deficiency of the Yamaguchi and Yamaguchi (Ref. 7) potentials has not been previously pointed out in the literature.

[21]S. Kikuchi, J. Sanda, S. Sowa, I. Hayashi, K. Nisimura, and K. Fukinaga, J. Phys. Soc. Japan 15, 9 (1960).

[22]J. D. Seagrave, Phys. Rev. 97, 757 (1955).

[23]S. W. Bunker, J. M. Cameron, R. F. Carlson, J. R. Richardson, P. Thomăs, W. T. H. Van Oers, and J. Verba, Nucl. Phys. A113, 461 (1968).

[24]J. H. Williams and M. K. Brussel, Phys. Rev. 110, 136 (1958).

[25]J. T. Holdeman and R. M. Thaler, Phys. Rev. 139, B1186 (1965).

[26]J. C. Faivre, D. Garreta, J. Jungerman, A. Papineau, J. Sura, and A. Tarrats, Nucl. Phys. A127, 169 (1969).

[27]H. E. Conzett, H. S. Goldberg, E. Shield, R. J. Slobodrian, and S. Yombe, Phys. Rev. Letters 11, 68 (1964).

[28]A comparison by Sloan (Ref. 4) of the unitary-model partial-wave amplitudes with those computed by an exact integration of the Faddeev equations for central S-wave forces [Ref. 4 and R. Aaron, R. D. Amado, and Y. Y. Yam, Phys. Rev. 140, B1291 (1965)] suggests that only the amplitudes for small J are in serious error and that for larger J (perhaps $J \geq \frac{7}{2}$) the amplitudes obtained from the unitary model, or indeed, a nonunitarized impulse calculation, will be reliable.

[29]H. Kottler and K. L. Kowalski, Phys. Rev. 138, B619 (1965).

[30]Sloan (Ref. 4) has demonstrated this by comparing exact and unitary-model results for S-wave-potential models.

[31]G. F. Chew, Phys. Rev. 80, 196 (1950). In K. L. Kowalski and S. C. Pieper, Phys. Rev. C 4, 74 (1971) we have shown that for an S-wave separable-potential model the fixed-scatterer approximation is reliable at these energies in the forward direction.

[32]The results of R. W. Peacock and R. D. Purrington, Phys. Rev. C 4, 281 (1971) lend some support to this contention, since they find that two separable potentials with substantially different off-shell behavior yield, in an exact calculation, essentially equal N-d scattering amplitudes (with the exception of the $^2S_{1/2}$ amplitude).

[33]The results mentioned in Ref. 28 show that for an "exact" calculation, the partial-wave amplitudes for large J may still be computed using a form of the impulse approximation. The angular momentum analysis developed in Sec. II will be useful for such calculations and, indeed, this was one of the primary motivations for presenting this analysis.

[34]An approximation recently proposed by Sloan [I. H. Sloan, Separable Expansions and Perturbation Theory for Three-Body Collisions (to be published) and K. L. Kowalski and S. C. Pieper, following paper, Phys. Rev. C 5, 324 (1972)] may allow the perturbative computation of N-d polarization without including the P waves in an exact integration of the three-particle equations.